Journal of Power Sources 196 (2011) 5485–5489

Contents lists available at ScienceDirect

Journal of Power Sources

journal homepage: www.elsevier.com/locate/jpowsour

Short communication

Energy efficiency of a microtubular solid-oxide fuel cell

Toshio Suzuki[a,*], Shinichi Sugihara[b], Koichi Hamamoto[a], Toshiaki Yamaguchi[a], Yoshinobu Fujishiro[a]

[a] National Institute of Advanced Industrial Science and Technology (AIST), Nagoya, Japan
[b] Mazda Motor Corporation, Yokohama, Japan

ARTICLE INFO

Article history:
Received 27 January 2011
Received in revised form 18 February 2011
Accepted 18 February 2011
Available online 26 February 2011

Keywords:
SOFC
Efficiency
Hydrogen
Microtubular

ABSTRACT

Energy efficiency of a single solid-oxide fuel cell (SOFC) has been studied in various experimental conditions and directly correlated to the character of the cell. A microtubular cell, which has the exact geometry for stack/module application, is used for this study. The energy efficiency simply improves by increasing the operating temperature, and reaches over 40% (lower heating value: LHV) at the operating temperature of over 700 °C in flowing 20% H_2–Ar fuel inside the tube. Impedance analysis has shown that the gas transport is the limiting factor for improving the energy efficiency at lower operating temperatures.

1. Introduction

Environmental and energy issues have never been so much discussed in the 21st century. In addition to reducing CO_2 emission, wisely use of energy resources is highly demanded because simply they (even nuclear energy) are limited. Thus, efficiency is one of very important keywords for the energy-consuming related issues. There is no doubt that one of most priority energy resources is fossil fuel because the human races holds quite large amount of the resources; and this is where solid oxide fuel cells (SOFCs) play an important role due to their high energy conversion efficiency [1–5]. Because the SOFCs are operated at relatively high temperatures between 500 and 1000 °C; it is possible to utilize the heat to steam-reform hydrocarbon fuel internally; resulting in producing hydrogen,

$$2CH_4 + 2H_2O \rightarrow 2CO + 6H_2 \quad (1)$$

If one compares to the partial oxidation of the hydrocarbon fuel,

$$2CH_4 + O_2 \rightarrow 2CO + 4H_2 \quad (2)$$

It can be seen that hydrogen is effectively produced utilizing steam-reforming reaction in Eq. (1). Note that the reaction in Eq. (1) is endothermic which requires heat to proceed the reaction.

So far, development of SOFCs has been mainly focused on the materials for an electrolyte, anode and cathode, and tremendous amount of studies have been reported [6–11]. Cell performance strongly depends upon, not only the kind of materials but also microstructure of electrodes, gas flow geometry (stack/module design) [12], and thus, it is difficult to discuss the energy efficiency from the single cell measurements, simply because the cell testing set-up would be different from stack–module configuration.

Energy efficiency of SOFCs is given by as follows using the value of lower heating value (LHV),

$$\text{Efficiency (LHV)} = \frac{U_f \times \eta_{operation}}{1.25}, \quad (3)$$

where U_f, and $\eta_{operation}$ are fuel utilization and cell operating voltage. U_f can be give by

$$U_f = \frac{I_{operation}}{4Fu}, \quad (4)$$

where $I_{operation}$, F and u are operating current density, Faraday constant, and H_2 flow rate per electrode area (mL s^{-1} cm^{-2}), respectively.

The purpose of this paper is to show the influence of operating conditions on the energy efficiency of a single cell in order to understand the determining factors of fuel cell efficiency on the single cell, and to feedback to the cell manufacturing process for the improvement of SOFCs towards earlier commercialization. In this study, micro tubular design [13–16] was selected; the anode fuel gas flow geometry is defined by the cell structure, not by gas manifold as the planar type cell is. This means that the results of single cell can be directly applied to stack/module design, leading to high efficient SOFC modules and systems.

* Corresponding author. Tel.: +81 52 736 7083; fax: +81 52 736 7405.
E-mail address: toshio.suzuki@aist.go.jp (T. Suzuki).

0378-7753/$ – see front matter © 2011 Elsevier B.V. All rights reserved.
doi:10.1016/j.jpowsour.2011.02.052

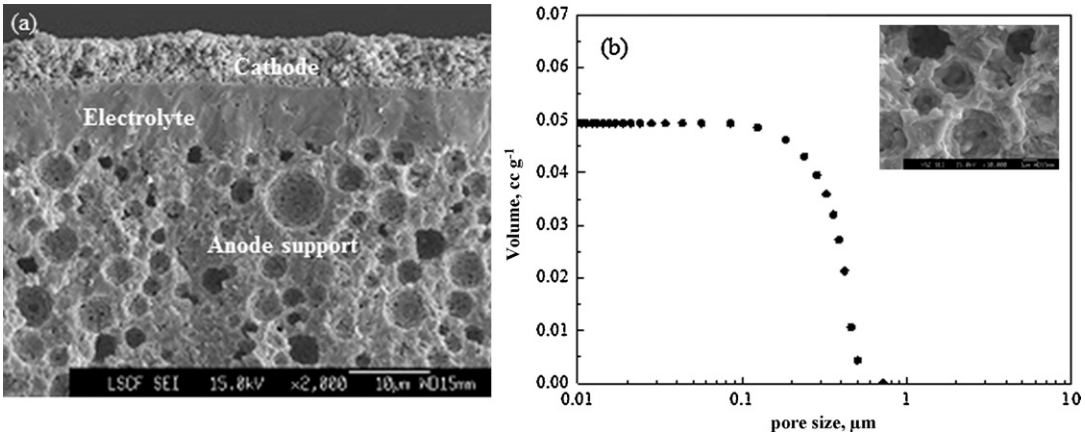

Fig. 1. Cross-sectional fracture SEM images of (a) a micro tubular SOFC and (b) the cumulative pore volume of the anode support before the test.

2. Experimental

The micro tubular SOFC's we report here consist of nickel–yttria stabilized zirconia (Ni/YSZ) for the anode, scandia stabilized zirconia (ScSZ) for the electrolyte, and $La_{0.6}Sr_{0.4}Co_{0.2}Fe_{0.8}O_3$ – gadolinia doped ceria (LSCF/GDC) for the cathode, with an inter-layer of GDC between the cathode and the electrolyte. Note that all materials used for the SOFC fabrication are commercially available.

2.1. Fabrication

Anode tubes were made from nickel oxide (NiO) powder (Sumitomo Mining Co., Ltd.), yttrium stabilized zirconia (YSZ) (8YSZ, Tosoh Co., Ltd.), poly methyl methacrylate beads (PMMA) (Sekisui Plastics Co., Ltd.), and cellulose (Yuken Kogyo Co., Ltd.). These powders were mixed for 1 h by a mixer 5DMV-r (Dalton Co., Ltd.), and after adding the correct amount of water, were stirred for 30 min in a vacuumed chamber. The mixture that was prepared from these powders was left over 15 h for aging. The tubes were extruded, using the aforementioned extrudate, from a metal mold (2.4 mm diameter with 2.0 mm diameter pin) by using a piston cylinder type extruder (Ishikawa-Toki Tekko-sho Co., Ltd.). A slurry for dip-coating the electrolyte was prepared by mixing the scandium stabilized zirconia (ScSZ) powder (Daiichiki-genso Co., Ltd.), solvents (toluene and ethanol), binder (poly vinyl butyral), dispersant (polymer of an amine system) and plasticizer (dioctyl phthalate) for 24 h. The anode tubes were dipped in the slurry and coated at the pulling rate of 1.0 mm s^{-1}. The coated films were dried in air, and co-sintered at 1350 °C for 1 h in air. An inter-layer slurry of gadolinia doped ceria (GDC) (Shinteu Kagaku Co., Ltd.) was dip-coated on the electrolyte layer of the tube and sintered at 1100 °C. A cathode slurry of $La_{0.6}Sr_{0.4}Co_{0.2}Fe_{0.8}O_{3-y}$ (LSCF) and the GDC powder (LSCF/GDC)

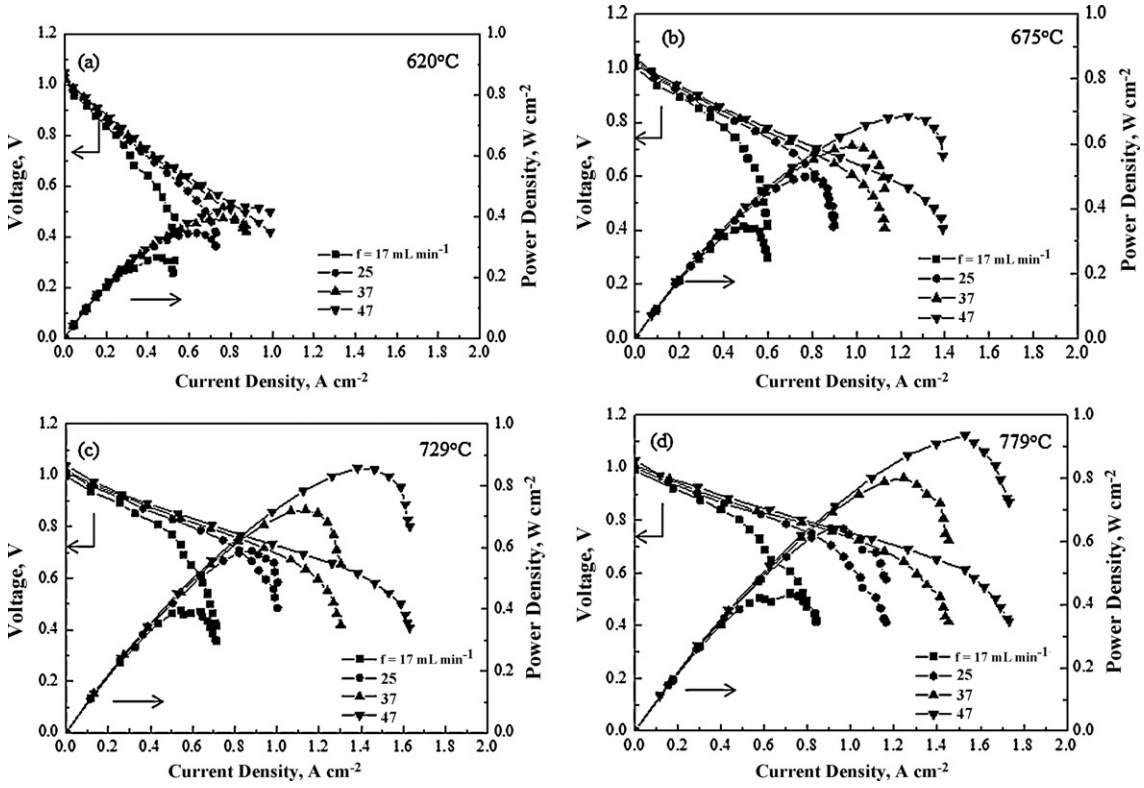

Fig. 2. Cell performance at various fuel flow rates at (a) 620 °C, (b) 675 °C, (c) 729 °C, and (d) 779 °C.

were dip-coated on the inter-layer. The SOFCs were completed by sintering at 1050 °C.

2.2. Characterization

The microstructure of the electrodes of the tubular cell was observed by using a mercury porosimeter and a scanning electron microscopy (SEM) (JEOL, JSM6330F). The electrochemical cell performance was investigated by using a potentiostat (Solartron 1296) and impedance analyzer at the cell temperature of 620, 675, 729 and 779 °C, respectively, which were monitored by a thermocouple placed closed to the sample. The size of the cell was 1.8 mm in diameter and 30 mm in length with cathode length of 11 mm, and an effective electrode area of 0.56 cm^2. Ag wire was used for collecting current from the anode and cathode sides, which were both fixed using Ag paste. The current collection from the anode side was made from an edge of the anode tube, and the collection from the cathode side was made from the whole cathode area. Detailed information for experimental setup can be found in previous literature [17]. Diluted Hydrogen (20% H_2 in Ar) was flowed inside of the tubular cell at a flow rate of 17–47 mL min^{-1} (H_2 flow rate: 6.1–16.8 mL min^{-1}/electrode area of 1 cm^2). Dilute hydrogen can be considered as steam-reformed hydrocarbon fuel gas. Air was supplied at the cathode side at a flow rate of 100 mL min^{-1}.

3. Results and discussion

Fig. 1(a) and (b) show cross-sectional fracture SEM image of a micro tubular SOFC and pore distribution of the anode tube before reduction (oxide state). As can be seen in Fig. 1(a), large pores of about 3–5 μm are well distributed, however, the main pore size of the anode is about 0.2 μm from the mercury porosimeter measurement in Fig. 1(b), which is corresponding to pores between grains. The porosity of the anode tube was 22% before reduction.

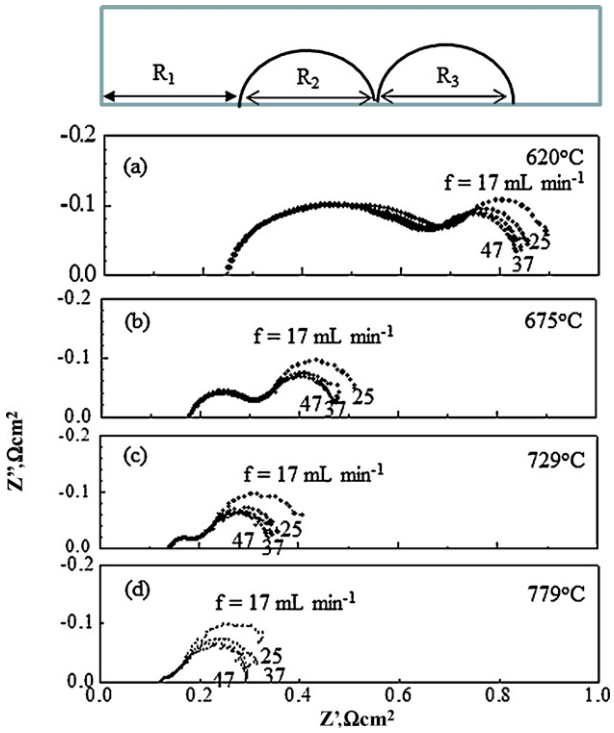

Fig. 3. Impedance spectra of the cell obtained at various flow rates at (a) 620 °C, (b) 675 °C, (c) 729 °C, and (d) 779 °C.

Fig. 2 show the performance of the microtubular cell at various fuel flow rates at (a) 620 °C, (b) 675 °C, (c) 729 °C, and (d) 779 °C,

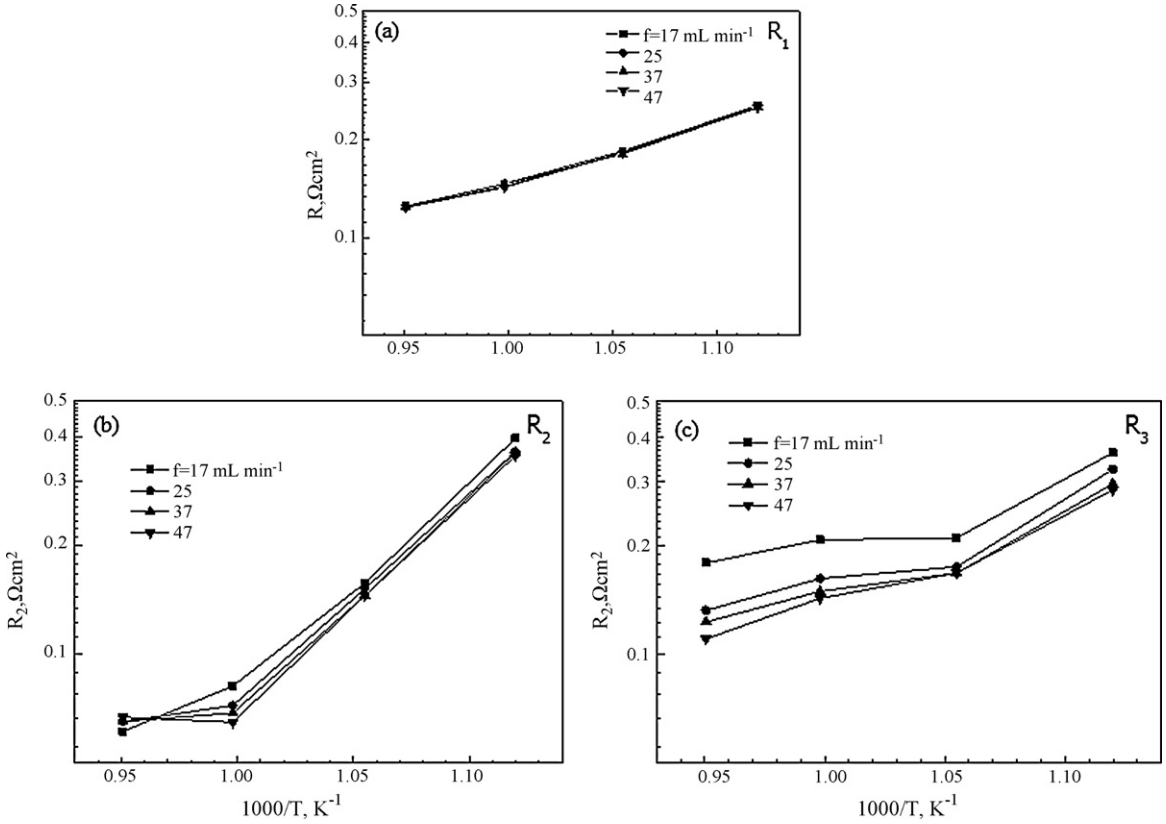

Fig. 4. Temperature dependent ohmic and overpotential resistances at various flow rates for (a) R_1, (b) R_2, and (c) R_3.

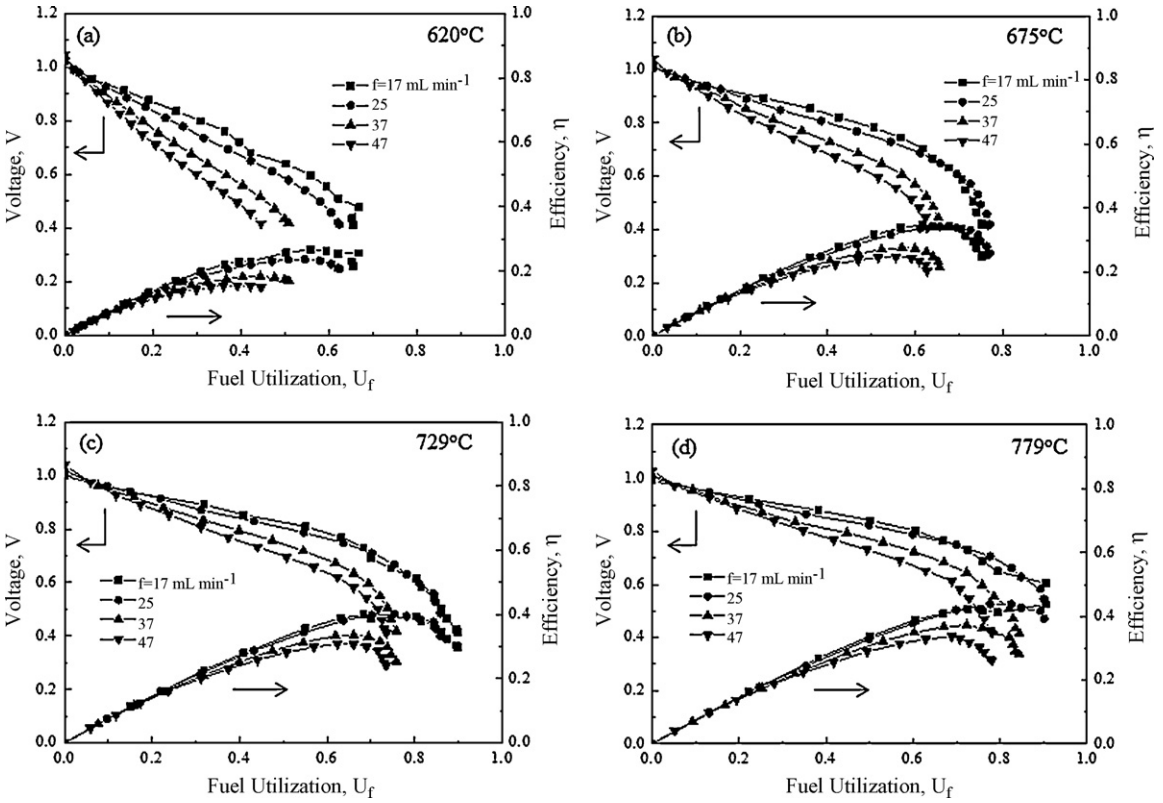

Fig. 5. Energy efficiency of the single cell at various flow rates at (a) 620 °C, (b) 675 °C, (c) 729 °C, and (d) 779 °C.

respectively. As can be seen, the maximum power density increases as the fuel gas flow increases, from 0.25 to 0.4 W cm^{-2} at 620 °C and from 0.4 to 0.9 W cm^{-2} at 779 °C. It can be seen that almost all data shows that the maximum power density is limited by concentration polarization due to low fuel concentration region. Also, it is observed that the performance of the cell at low current density region decreased as the gas flow rate decreased. To understand this phenomenon, impedance analysis was employed near the open circuit voltage (OCV).

Fig. 3 shows impedance spectra of the cell obtained at various flow rates at (a) 620 °C, (b) 675 °C, (c) 729 °C, and (d) 779 °C, respectively. As clearly be seen, the effect of the gas flow rate was observed in the low frequency semi-circle (R_3), which is corresponding to gas transport [18]. The feature of this sample with 22% anode porosity turned out to have relatively high polarization resistance compared to the charge transfer resistance (R_2) at higher operating temperatures. Fig. 4 shows the plots of each resistance (R_1, R_2 and R_3) as a function of reciprocal temperature for various fuel gas flow rates. It was shown that R_1 and R_2 showed small influence of fuel gas flow rate, while R_3 shows strong influences. The slope of the R_3 vs. $1/T$ plot shown in Fig. 4(c) also changed as the temperature changed, indicating that multiple processes of the gas transport could be existed, possibly related to H_2 diffusion into the anode and H_2O diffusion out of the anode.

Fig. 5 shows energy efficiency of the single cell at various flow rates at (a) 620 °C, (b) 675 °C, (c) 729 °C, and (d) 779 °C, respectively. The energy efficiency turned out to be better for lower fuel gas flow rate for all measured temperatures, and reached over 40% at 729 °C or higher cell temperatures. Note that the fuel (H_2) used in this study was diluted to 20% in Ar, and the thus fuel concentration at 80% fuel utilization would be only 4% H_2. Thus the energy efficiency of the cell is expected to be higher for actual cell operating condition.

Fig. 6 shows maximum energy efficiency at each operating temperature vs. the resulting power density. As can be seen, the energy efficiency strongly depends upon the power density which is controlled by fuel gas flow rate. In order to improve the energy efficiency, the output power needs to be reduced, and operating SOFC in higher temperature results in realizing higher energy efficiency. These results can be used for designing stack/module size as well as the system specification. After all, lowering the operating temperature is still a challenging issue from the energy efficiency point of view. It was shown that the limiting factor for improving energy efficiency at lower operating temperatures was mainly due to performance drop in higher fuel utilizing condition, related to the gas diffusion process. Thus, it can be said that improving the

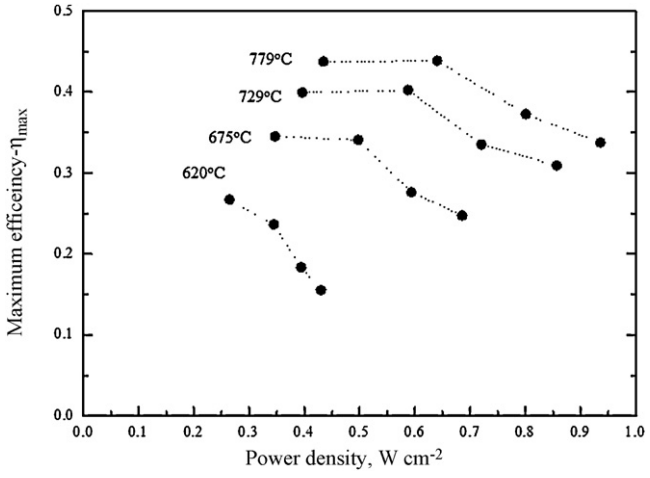

Fig. 6. Maximum energy efficiency at each operating temperature.

anode microstructure could be a key for the development of SOFCs towards the commercialization.

4. Conclusions

Energy efficiency of a microtubular SOFC was studied in various experimental conditions in order to understand the limiting factor for improving SOFC performance at lower operating temperature. A microtubular cell used for this study, which was also the exact cell for stack/module fabrication, consisted of Ni/YSZ for the anode, ScSZ for the electrolyte, GDC for the interlayer, and LSCF/GDC for the cathode, respectively. The energy efficiency simply increased as the operating temperature increased, and reached over 40% (LHV) at the operating temperature of over 700 °C in flowing 20% H_2–Ar fuel inside the tube. Impedance analysis showed that the improvement of energy efficiency at higher temperatures was mainly correlated to the decrease of the gas transport polarization resistance. After all, the single cell showed that over 40% of energy efficiency at 729 °C or higher using the anode microstructure in the microtubular SOFCs. Further development of fabrication technique for improving electrode microstructure is expected in order to improve the energy efficiency at lower operating temperatures.

References

[1] N.Q. Minh, J. Am. Ceram. Soc. 78 (1993) 563–588.
[2] O. Yamamoto, Electrochim. Acta 45 (2000) 2423–2435.
[3] S.C. Singhal, Solid State Ionics 152–153 (2002) 405–410.
[4] B.C.H. Steele, A. Heinzel, Nature 414 (2001) 345–352.
[5] H. Yokokawa, N. Sakai, T. Horita, K. Yamaji, M.E. Brito, MRS Bull. 30 (2005) 591–595.
[6] J.W. Yan, H. Matsumoto, M. Enoki, T. Ishihara, Electrochem. Solid-State Lett. 8 (2005) A389–A391.
[7] Z.P. Shao, S.M. Haile, Nature 431 (2004) 170–173.
[8] S.W. Tao, J.T.S. Irvine, Nat. Mater. 2 (2003) 320–323.
[9] K. Eguchi, T. Setoguchi, T. Inoue, H. Arai, Solid State Ionics 52 (1992) 165–172.
[10] T. Hibino, A. Hashimoto, K. Asano, M. Yano, M. Suzuki, M. Sano, Electrochem. Solid-Sate Lett. 5 (2002) A242–A244.
[11] E.D. Wachsman, Solid State Ionics 152 (2002) 657–662.
[12] T. Suzuki, M.H. Zahir, Y. Funahashi, T. Yamaguchi, Y. Fujishiro, M. Awano, Science 325 (2009) 852–855.
[13] N.M. Sammes, Y. Du, R. Bove, J. Power Sources 145 (2005) 428–434.
[14] K. Kendall, M. Palin, J. Power Sources 71 (1998) 268–270.
[15] K. Yashiro, N. Yamada, T. Kawada, J. Hong, A. Kaimai, Y. Nigara, J. Mizusaki, Electrochemistry 70 (2002) 958–960.
[16] T. Suzuki, Y. Funahashi, T. Yamaguchi, Y. Fujishiro, M. Awano, Electrochem. Solid-Sate Lett. 10 (2007) A177–A179.
[17] T. Suzuki, T. Yamaguchi, Y. Fujishiro, M. Awano, J. Electrochem. Soc. 153 (2006) A925–A928.
[18] S.B. Adler, Solid State Ionics 111 (1998) 125.